Possible charmed-strange molecular pentaquarks in quark delocalization color screening model

Xuejie Liu,[1,†] Yue Tan,[2,‡] Xiaoyun Chen,[5,§] Dianyong Chen,[3,6,*] Hongxia Huang,[4,‖] and Jialun Ping[4,¶]

[1]*School of Physics, Henan Normal University, Xinxiang 453007, People's Republic of China*
[2]*School of Mathematics and Physics, Yancheng Institute of Technology, Yancheng, 224051, People's Republic of China*
[3]*Lanzhou Center for Theoretical Physics, Lanzhou University, Lanzhou 730000, People's Republic of China*
[4]*Department of Physics, Nanjing Normal University, Nanjing 210023, People's Republic of China*
[5]*College of Science, Jinling Institute of Technology, Nanjing 211169, People's Republic of China*
[6]*School of Physics, Southeast University, Nanjing 210094, People's Republic of China*

(Received 21 August 2023; accepted 11 October 2023; published 6 November 2023)

Inspired by the observations of $T^a_{c\bar{s}0}(2900)^0$ and $T^a_{c\bar{s}0}(2900)^{++}$ by LHCb Collaboration, we perform a systematical investigation of the charmed-strange pentaquark system by using the resonance group method in the quark delocalization color screening model. The present estimations indicate the existence of two bound states with $I(J^P)$ to be $\frac{1}{2}(\frac{5}{2}^-)$ and $\frac{3}{2}(\frac{5}{2}^-)$, and the masses are predicted to be 3392 and 3307 MeV, respectively. Moreover, three resonance states are also predicted in the present work. The $\Sigma_c K^*$ resonance with $I(J^P) = \frac{1}{2}(\frac{1}{2}^-)$ could be observed in the ND_s^*, $\Lambda_c K^*$ and $\Sigma_c K$ channels, the mass and width are estimated to be (3342–3346) MeV and 25.5 MeV, respectively. The $\Sigma_c K^*$ resonance with $I(J^P) = \frac{1}{2}(\frac{3}{2}^-)$ is available only in the $\Sigma_c^* K$ channel, and the resonance parameters are evaluated to be $m_R = 3333$ MeV and $\Gamma_R = 3.3$ MeV. We also find a very narrow ΔD_s^* resonance state in the $\Sigma_c K$ channel with $I(J^P) = \frac{3}{2}(\frac{1}{2}^-)$ and $m_R = 3343$ MeV. These predictions of the charmed-strange pentaquark may be accessible by further experimental measurements in Belle II and LHCb Collaborations, and the corresponding experimental measurements can in turn be a good test of present estimations.

DOI: 10.1103/PhysRevD.108.094008

I. INTRODUCTION

The concept of multiquark states was proposed at the inception of the quark model [1,2]. With the improvement of experimental equipment and techniques, an increasing number of new hadron states have been observed experimentally since the observation of $X(3872)$ in 2003 [3]. Among these new hadron states, the charged charmoniumlike states are particular interesting, such as the first confirmed charged charmoniumlike state $Z_c(3900)$ [4,5], which certainly could not be conventional hadrons. These experimental observations provide us with an excellent opportunity to search for multiquark states and some progress has been made [6–12].

Besides the charmoniumlike states, an increasing number of charmed-strange-mesonlike states have also been observed in the recent two decades. As early as the year of 2003, the *BABAR* Collaboration reported a narrow peak, $D_{s0}^*(2317)$, in the $D_s^+\pi$ invariant mass spectrum [13,14]. Later, the CLEO Collaboration [15] confirmed the existence of this state and further reported another state $D_{s1}(2460)$ in the $D_s^*\pi$ invariant mass distribution. Moreover, the existence of the $D_{s0}^*(2317)$ and $D_{s1}(2460)$ had also been confirmed by the Belle [16,17] and *BABAR* Collaborations [18,19]. In addition, in the year 2018, the BESIII Collaboration detected $D_{s0}^*(2317)$ by the observation of the process $e^+e^- \to D_s^{*+}D_{s0}^*(2317) + \text{c.c.}$ [20]. Noted that the masses of $D_{s0}^*(2317)$ and $D_{s1}(2460)$ are far below the theoretical predictions of the masses of charmed-strange mesons with $J^P = 0^+$ and $J^P = 1^+$, this inconsistency between the quark model expectations and experimental measurements makes these two states unlike to be conventional charmed-strange mesons. In this case, some exotic interpretations have been proposed, such as the tetraquark states [21–26], the

*Corresponding author: chendy@seu.edu.cn
†1830592517@qq.com
‡tanyue@ycit.edu.cn
§xychen@jit.edu.cn
‖hxhuang@njnu.edu.cn
¶jlping@njnu.edu.cn

molecular interpretations, where the $D_{s0}^*(2317)$ and $D_{s1}(2460)$ were assigned as DK and D^*K molecular states [27–36], respectively, and the mixture of charmed strange mesons and tetraquark states [37,38].

The search for exotic states with charmness and strangeness still goes on. In the year 2020, the LHCb Collaboration reported two fully open-flavor tetraquark candidates, $X_0(2900)$ and $X_1(2900)$, in the invariant mass distribution of D^-K^+ of the process $B^\pm \to D^+D^-K^\pm$ [39,40]. Since they are observed in the D^-K^+ spectrum, their minimal quark components are $ud\bar{c}\,\bar{s}$. To reveal the nature of $X_0(2900)$ and $X_1(2900)$, some different theoretical explanations have been proposed, such as the hadronic molecule states composed of $D^*\bar{K}^*$ or $D_1\bar{K}$ [41–44], compact tetraquark states [45–54], threshold effects [55,56] and so on.

Very recently, the LHCb Collaboration reported their observation of two new tetraquark candidates, $T^a_{c\bar{s}0}(2900)^0$ and $T^a_{c\bar{s}0}(2900)^{++}$,[1] in the $B^0 \to \bar{D}^0D_s^+\pi^-$ and $B^+ \to D^-D_s^+\pi^+$ decays [58,59]. From the observed channels, the least quark contents of these two states were $c\bar{s}n\bar{n}$, $n = (u, d)$, which are similar to those of $X_0(2900)$ and $X_1(2900)$. The properties of such kinds of open flavor states have been researched in the literature [42,50,60–64] before the experimental observations, and after the discovery of $T^a_{c\bar{s}0}(2900)$, the mass [65–69], and decay properties have been further investigated [70–73].

The observations of $T^a_{c\bar{s}0}(2900)$, together with $D_{s0}^*(2317)$, $D_{s1}(2460)$ and $X_{0,1}(2900)$ make the exotic candidates around the thresholds of a charmed meson and a strange meson abundant. Similar to the meson-meson case, there may also exist exotic candidates around the threshold of a charmed baryon and a strange meson, which could be $c\bar{s}nnn$ pentaquark states. Some investigations of $c\bar{s}nnn$ pentaquark states have been presented in the literature, for example, in Ref. [67], the $\Lambda_cK^{(*)}$ and $\Sigma_cK^{(*)}$ interactions were investigated by one-boson-exchange effective potentials and four possible charmed strange molecular pentaquark states were predicted. In Ref. [74], a systematic estimation of $c\bar{s}nnn$ pentaquark states had been performed and the authors suggested searching such kind of pentaquark states in the bottom hadron decays.

In the present work, we systematically investigate the $c\bar{s}nnn$ system in a quark delocalization color screening model (QDCSM), where the effective potential between two hadrons with different quantum numbers are evaluated, and then we attempt to find possible bound states by performing the bound calculations with coupled channel effects. Moreover, based on the conservation of the quantum numbers and the limitation of the phase space, we also check the possible strong decay channels of the charmed-strange pentaquark system and evaluate the existence of resonance states.

This work is organized as follows. In Sec. II, the detail of the QDCSM is presented. The numerical results for the effective potential, possible bound states, and resonances are given in Sec. III, and the last section is devoted to the summary.

II. THE QUARK DELOCALIZATION COLOR SCREENING MODEL

The QDCSM is an extension of the native quark cluster model [75–78] and was developed with the aim of addressing multiquark systems (More detail of QDCSM can be found in the Refs. [79–83]). In the QDCSM, the general form of the Hamiltonian for the pentaquark system is,

$$H = \sum_{i=1}^{5}\left(m_i + \frac{\boldsymbol{p}_i^2}{2m_i}\right) - T_{\rm CM} + \sum_{j>i=1}^{5} V(r_{ij}), \quad (1)$$

where the center-of-mass kinetic energy, $T_{\rm CM}$, is subtracted without losing generality since we mainly focus on the internal relative motions of the multiquark system. The two body potentials include the color-confining potential, $V_{\rm CON}$, one-gluon exchange potential, $V_{\rm OGE}$, and Goldstone-boson exchange potential, V_χ, respectively, i.e.,

$$V(r_{ij}) = V_{\rm CON}(r_{ij}) + V_{\rm OGE}(r_{ij}) + V_\chi(r_{ij}). \quad (2)$$

Noted herein that the potentials include the central, spin-spin, spin-orbit, and tensor contributions, respectively. Since the current calculation is based on S-wave, only the first two kinds of potentials will be considered attending the goal of the present calculation and for clarity in our discussion. In particular, the one-gluon-exchange potential, $V_{\rm OGE}(r_{ij})$, reads,

$$V_{\rm OGE}(r_{ij}) = \frac{1}{4}\alpha_{ij}\boldsymbol{\lambda}_i^c\cdot\boldsymbol{\lambda}_j^c \times\left[\frac{1}{r_{ij}} - \frac{\pi}{2}\delta(\boldsymbol{r}_{ij})\left(\frac{1}{m_i^2}+\frac{1}{m_j^2}+\frac{4\boldsymbol{\sigma}_i\cdot\boldsymbol{\sigma}_j}{3m_im_j}\right)\right], \quad (3)$$

where m_i is the quark mass, $\boldsymbol{\sigma}$ and $\boldsymbol{\lambda}^c$ are the Pauli matrices and SU(3) color matrices, respectively. The QCD-inspired effective scale-dependent strong coupling constant, α_{ij}, offers a consistent description of mesons and baryons from the light to the heavy quark sectors. Their values are associated with the quark flavor and determined by the mass difference of the hadrons. It is worth mentioning that a conventional meson contains only one quark and one antiquark, while a baryon has three quarks, which suggests the existence of three-body interactions in the baryon system. Therefore, when using a simple two-body interaction to reproduce the meson and baryon spectrum in a nonrelativistic quark model with OGE potential, the

[1]Here, the LHCb naming scheme is employed [57], which has not been officially accepted.

parameter values $\alpha_{qq'}$ and $\alpha_{q\bar{q}'}$, which are determined individually by the baryon and meson spectrum individually, are not the same.

In the QDCSM, the confining interaction $V_{\rm CON}(r_{ij})$ can be expressed as

$$V_{\rm CON}(r_{ij}) = -a_c\boldsymbol{\lambda}_i^c\cdot\boldsymbol{\lambda}_j^c[f(r_{ij}) + V_{0_{ij}}], \tag{4}$$

where a_c represents the strength of the confinement potential and $V_{0_{ij}}$ refers to the zero-point potential. In the case of quark-quark interactions, the value of $V_{0_{qq}}$ is determined based on the differences between theoretical estimations and experimental measurements of baryon masses. This value is the same for quarks with different flavors. On the other hand, for quark-antiquark interactions, the value of $V_{0_{q\bar{q}}}$ is determined by reproducing the mass differences between theoretical estimations and experimental measurements of the meson masses, which is also flavor-independent. Moreover, in the quark delocalization color screening model, the quarks in the considered pentaquark state $c\bar{s}nnn$ are first divide into two clusters, which are baryon cluster composed of three quarks, and meson cluster composed of one quark and one antiquark. And then the five-body problem can be simplified as a two-body problem the $f(r_{ij})$ is,

$$f(r_{ij}) = \begin{cases} r_{ij}^2 & \text{if } i,j \text{ occur in the same cluster,} \\ \frac{1-e^{-\mu_{ij}r_{ij}^2}}{\mu_{ij}} & \text{if } i,j \text{ occur in different cluster,} \end{cases} \tag{5}$$

where the color screening parameter μ_{ij} is determined by fitting the deuteron properties, nucleon-nucleon, and nucleon-hyperon scattering phase shifts [81,84], with $\mu_{nn} = 0.45$ fm^{-2}, $\mu_{ns} = 0.19$ fm^{-2} and $\mu_{ss} = 0.08$ fm^{-2}, satisfying the relation $\mu_{ns}^2 = \mu_{nn}\mu_{ss}$, where n represents u or d quark. From this relation, a fact can be found that the heavier the quark, the smaller the parameter μ_{ij}. When extending to the heavy-quark case, there is no experimental data available, so we take it as an adjustable parameter. In Ref. [85], we investigate the mass spectrum of P_ψ^N with μ_{cc} varying from 10^{-4} to 10^{-2} fm^{-2}, and our estimation indicated that the dependence of the parameter μ_{cc} is not very significant.[2] In the present work, we take $\mu_{cc} = 0.01$ fm^{-2}. Then μ_{sc} and μ_{nc} are obtained by the relations $\mu_{sc}^2 = \mu_{ss}\mu_{cc}$ and $\mu_{nc}^2 = \mu_{nn}\mu_{cc}$, respectively. It should be noted that μ_{ij} are phenomenal model parameters, their values are determined by reproducing the relevant mass spectra and phase shifts of the scattering processes. In Ref. [81], the authors found that with the relation $\mu_{qs}^2 = \mu_{qq}\mu_{ss}$, the masses of the ground state baryons composed of light quarks could be well reproduced. Later on, such relations have been successfully applied to investigate the states with heavy quarks [85–87].

The Goldstone-boson exchange interactions between light quarks appear because of the dynamical breaking of chiral symmetry. The following π, K, and η exchange terms work between the chiral quark-(anti)quark pair, which read,

$$V_\chi(r_{ij}) = v_{ij}^\pi(r_{ij})\sum_{a=1}^{3}\lambda_i^a\lambda_j^a + v_{ij}^K(r_{ij})\sum_{a=4}^{7}\lambda_i^a\lambda_j^a + v_{ij}^\eta(r_{ij}) \times[(\lambda_i^8\cdot\lambda_j^8)\cos\theta_P - (\lambda_i^0\cdot\lambda_j^0)\sin\theta_P], \tag{8}$$

with

$$v_{ij}^B = \frac{g_{ch}^2}{4\pi}\frac{m_B^2}{12m_im_j}\frac{\Lambda_B^2}{\Lambda_B^2 - m_B^2}m_B \times\left\{(\boldsymbol{\sigma}_i\cdot\boldsymbol{\sigma}_j)\left[Y(m_Br_{ij}) - \frac{\Lambda_B^3}{m_B^3}Y(\Lambda_Br_{ij})\right]\right\}, \tag{9}$$

with $B = (\pi, K, \eta)$ and $Y(x) = e^{-x}/x$ to be the standard Yukawa function. $\boldsymbol{\lambda}^a$ is the SU(3) flavor Gell-Mann matrix. The masses of the η, K, and π meson are taken from the experimental value [88]. By matching the pion exchange diagram of the NN elastic scattering process at the quark level and at the hadron level, one can relate the πqq coupling with the one of πNN, which is [89,90],

[2]The typical size of the multiquark system should be several femtometres, for example, if the size of the multiquark system to be 2 fm, then one can find $\mu_{cc}r^2 \propto (10^{-4}$–$10^{-2})$, $\mu_{cn}r^2 = \sqrt{\mu_{cc}\mu_{nn}}r^2 \propto (10^{-2}$–$10^{-1})$ and $\mu_{cs}r^2 = \sqrt{\mu_{cc}\mu_{ss}}r^2 \propto (10^{-2}$–$10^{-1})$, thus the value of the $\mu_{ij}r^2$ is rather small when at least one charm quark included, and in this case, the exponential function can be approximated to be,

$$e^{-\mu_{ij}r_{ij}^2} = 1 - \mu_{ij}r_{ij}^2 + \mathcal{O}(\mu_{ij}^2r_{ij}^4). \tag{6}$$

Accordingly, the confinement potential between two clusters is approximated to be,

$$V_{\rm CON}(r_{ij}) = -a_c\boldsymbol{\lambda}_i^c\cdot\boldsymbol{\lambda}_j^c\left(\frac{1-e^{-\mu_{ij}\mathbf{r}_{ij}^2}}{\mu_{ij}} + V_{0_{ij}}\right) \approx -a_c\boldsymbol{\lambda}_i^c\cdot\boldsymbol{\lambda}_j^c(r_{ij}^2 + V_{0_{ij}}), \tag{7}$$

which is the same as the expression of two quarks in the same cluster. Thus, when the value of the μ_{cc} is very small, the screened confinement will return to the quadratic form, which is why the results are insensitive to the value of μ_{cc}.

TABLE I. The values of the model parameters. The masses of mesons take their experimental values.

	Parameter	Value
Quark masses	m_u (MeV)	313
	m_s (MeV)	573
	m_c (MeV)	1788
Confinement	a_c (MeV fm^{-2})	58.03
	$V_{0_{qq}}$ (fm^2)	−1.2883
	$V_{0_{q\bar{q}}}$ (fm^2)	−0.7432
OGE	α_{uu}	0.5652
	α_{us}	0.5239
	α_{uc}	0.4673
	$\alpha_{u\bar{s}}$	1.4275
	$\alpha_{s\bar{c}}$	1.1901
Goldstone boson	m_π (fm^{-1})	0.7
	m_K (fm^{-1})	2.51
	m_η (fm^{-1})	2.77
	Λ_π (fm^{-1})	4.2
	$\Lambda_{\eta/K}$ (fm^{-1})	5.2
Wave function	b (fm)	0.518

TABLE II. The masses of the ground baryons and mesons in the unit of MeV. Experimental values are taken from the Particle Data Group (PDG) [88].

	N	Δ	Λ	Σ	Σ^*	Ξ	Ξ^*
Model	939	1232	1122	1237	1360	1374	1496
Expt.	939	1232	1116	1189	1385	1318	1533
	Λ_c	Σ_c	Σ_c^*	K	K^*	D_s	D_s^*
Model	2286	2464	2489	495	815	2018	2064
Expt.	2286	2455	2520	495	895	1968	2112

$$\frac{g_{ch}^2}{4\pi} = \left(\frac{3}{5}\right)^2 \frac{g_{\pi NN}^2}{4\pi}\frac{m_{u,d}^2}{m_N^2}, \tag{10}$$

which assumes that the flavor SU(3) is an exact symmetry, and only broken by the masses of the strange quark. As for the coupling $g_{\pi NN}$, it was determined by the NN elastic scattering [90]. Besides, with the MINUIT program, we can determine a set of optimized parameters by fitting the masses of the ground state mesons and baryons in QDCSM. The model parameters are shown in Table I and the reproduced masses of the mesons and baryons are listed in Table II.

In QDCSM, the quark delocalization is realized by specifying the single-particle orbital wave function as a linear combination of left and right Gaussian basis, the single- particle orbital wave functions used in the ordinary quark cluster model reads,

$$\begin{aligned}
\psi_\alpha(\boldsymbol{s}_i,\epsilon) &= (\Phi_\alpha(\boldsymbol{s}_i) + \epsilon\Phi_\beta(\boldsymbol{s}_i))/N(\epsilon),\\
\psi_\beta(\boldsymbol{s}_i,\epsilon) &= (\Phi_\beta(\boldsymbol{s}_i) + \epsilon\Phi_\alpha(\boldsymbol{s}_i))/N(\epsilon),\\
N(\epsilon) &= \sqrt{1+\epsilon^2+2\epsilon e^{-s_i^2/4b^2}},\\
\Phi_\alpha(\boldsymbol{s}_i) &= \left(\frac{1}{\pi b^2}\right)^{\frac{3}{4}} e^{-\frac{1}{2b^2}(\boldsymbol{r}_\alpha-\frac{2}{5}\boldsymbol{s}_i)^2},\\
\Phi_\beta(-\boldsymbol{s}_i) &= \left(\frac{1}{\pi b^2}\right)^{\frac{3}{4}} e^{-\frac{1}{2b^2}(\boldsymbol{r}_\beta+\frac{3}{5}\boldsymbol{s}_i)^2},
\end{aligned} \tag{11}$$

with $\boldsymbol{s}_i$, $i = (1, 2, \ldots, n)$, to be the generating coordinates, which are introduced to expand the relative motion wave function [91–93]. The parameter b indicates the size of the baryon and meson clusters, which is determined by fitting the radius of the baryon and meson by the variational method [94]. In addition, The mixing parameter $\epsilon(s_i)$ is not an adjusted one but is determined variationally by the dynamics of the multiquark system itself. This assumption allows the multiquark system to choose its favorable configuration in the interacting process. It has been used to explain the crossover transition between the hadron phase[3] and the quark-gluon plasma phase [80,83,95]. Due to the effect of the mixing parameter $\epsilon(s_i)$, there is a certain probability for the quarks between the two clusters to run, which leads to the existence of color octet states for the two clusters. Therefore, this model also includes the hidden color channel effect, which is confirmed by Refs. [96,97].

III. RESULTS AND DISCUSSIONS

In this work, we perform a systematical investigation of the low-lying charmed-strange pentaquark systems within the QDCSM. In the single channel calculations, if there is a strong attraction between two involved hadrons, a bound state or a resonance state is likely formed. Going to the multichannel coupling calculations, a bound state is shown if the energy of the state is below the threshold of the lowest channel and the thresholds of multibody decay channels, such as the deuteron in the two-channel coupling calculation of NN and $\Delta\Delta$ with $I(J^P) = 0(1^+)$ [83]. A resonance state is one that is a bound state in the single-channel calculation, but its energy is higher than the thresholds of some open channels. When the state is coupled to these open channels, it will decay strongly to these open channels and turn to a resonance state. In the scattering calculation of the open channel incorporating the resonance state, the phase shifts will be a structure in the region of the

[3]The phase shift of NN interaction could be described with the formalisms with hadrons only. After including the pseudoscalar, vector, and scalar meson, especially the σ meson, the NN interaction has been well described. In Ref. [80], the authors concluded that the σ-meson exchange can be replaced by quark delocalization and color screening mechanism introduced by QDCSM by comparing the NN scattering and deuteron properties obtained by chiral quark model and QDCSM.

TABLE III. The relevant channels for all possible states with different J^P quantum numbers.

	$I=\frac{1}{2}$					$I=\frac{3}{2}$		
$S=\frac{1}{2}$	ND_s Σ_cK	ND_s^* Σ_cK^*	Λ_cK $\Sigma_c^*K^*$	Λ_cK^*	ΔD_s^*	Σ_cK	Σ_cK^*	$\Sigma_c^*K^*$
$S=\frac{3}{2}$	ND_s^* $\Sigma_c^*K^*$	Λ_cK^*	Σ_cK^*	Σ_c^*K	ΔD_s $\Sigma_c^*K^*$	ΔD_s^*	Σ_cK^*	Σ_c^*K
$S=\frac{5}{2}$	$\Sigma_c^*K^*$				ΔD_s^*	$\Sigma_c^*K^*$		

resonance energy, such as $d^*(2380)$ in the two-channel calculation of D-wave NN and $\Delta\Delta$ with $I(J^P)=0(3^+)$ [98].

For the $c\bar{s}nnn$, $n=(u,d)$, pentaquark system, we only consider the S–wave channels with the spin $S=1/2,3/2$ and $5/2$, respectively. In the present work, we mainly focus on the pentaquark states in the molecular scenario, where the pentaquark states are composed of a baryon cluster and a meson cluster. Considering the color structure of these two clusters, both the color singlet-singlet $(1_c\otimes 1_c)$ and the color octet-octet $(8_c\otimes 8_c)$ channels should be involved in principle. However, as indicated in Ref. [83], the color screening confinement in Eq. (5) could be considered as an effective description of the color octet-octet channels (also known as the hidden color channels). Thus, only the color singlet-singlet channels are taken into consideration in the present estimations, and all the possible channels involved are collected in Table III.

A. The effective potentials

To search the possible bound states and resonance states composed of the hadron pair listed in Table III, we estimate the effective potentials between these hadron pairs for the first step. Here the definition of potential can be written as

$$E(S_m)=\frac{\langle\Psi_{5q}(S_m)|H|\Psi_{5q}(S_m)\rangle}{\langle\Psi_{5q}(S_m)|\Psi_{5q}(S_m)\rangle}, \tag{12}$$

where S_m stand for the distance between two clusters. $\Psi_{5q}(S_m)$ represents the wave function of a certain channel. Besides, $\langle\Psi_{5q}(S_m)|H|\Psi_{5q}(S_m)\rangle$ and $\langle\Psi_{5q}(S_m)|\Psi_{5q}(S_m)\rangle$ are the Hamiltonian matrix and the overlap of the states. So the effective potential between two colorless clusters is defined as,

$$V(S_m)=E(S_m)-E(\infty), \tag{13}$$

where $E(\infty)$ stand for at a sufficient large distance of two clusters. The estimated potentials for $I=1/2$ and $I=3/2$ are presented in Figs. 1 and 2, respectively.

As shown in Fig. 1, for the case of $I(J^P)=\frac{1}{2}(\frac{1}{2}^-)$, the potentials for the $\Sigma_c^*K^*$, Σ_cK^*, ND_s, and ND_s^* channels are attractive, while the potentials for the Λ_cK, Λ_cK^* and Σ_cK channels are repulsive. In particular, the potentials for $\Sigma_c^*K^*$ and Σ_cK^* channels are deeper than those of ND_s and ND_s^* channels, which indicates that the $\Sigma_c^*K^*$ and Σ_cK^* are more likely to form bound states or resonant states. For the case of $I(J^P)=\frac{1}{2}(\frac{3}{2}^-)$, the potentials of the Σ_cK^*, $\Sigma_c^*K^*$ and ND_s^* channels are attractive, while the potentials for the other two channels are repulsive. the attraction of Σ_c and K^* is much stronger than that of $\Sigma_c^*K^*$ and ND_s^*, which implies that it is possible for Σ_cK^* to form a bound or resonance

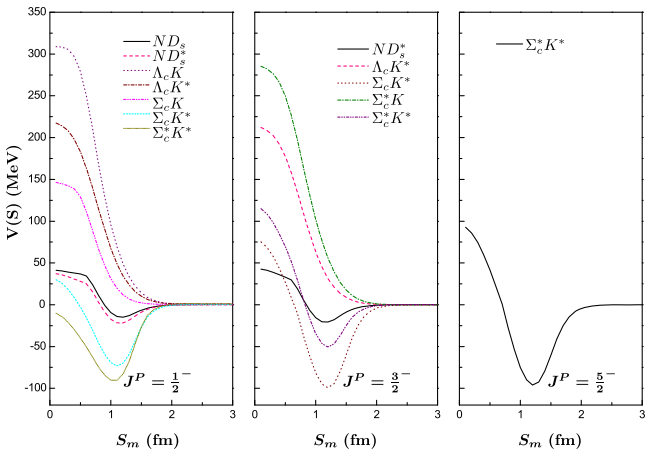

FIG. 1. The effective potentials defined in Eq. (13) for different channels of the charmed-strange pentaquark systems with $I=1/2$ in QDCSM.

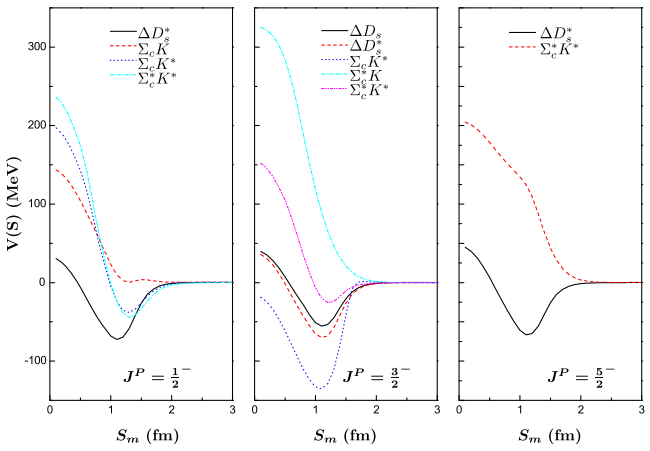

FIG. 2. The effective potentials defined in Eq. (13) for different channels of the charmed-strange pentaquark systems with $I=3/2$ in QDCSM.

state. For the $I(J^P) = \frac{1}{2}(\frac{5}{2}^-)$, the only possible channel is $\Sigma_c^* K^*$, and the potential is strongly attractive, which implies the possible bound state or resonance state in this channel.

In Fig. 2, we present the potentials of the channels with $I = 3/2$ but with different total angular momentum. For the case of $J^P = \frac{1}{2}^-$, one can find that the potentials are attractive for the channels ΔD_s^*, $\Sigma_c K^*$ and $\Sigma_c^* K^*$. The potential for $\Sigma_c K$ channel is repulsive, so no bound state or resonance states can be formed in this channel. However, the bound states or resonance states are possible for other channels due to the attractive nature of these interactions between the two clusters. Moreover, our estimations also indicate that the attraction between Δ and D_s^* is greater than the other channel, while, the potentials for $\Sigma_c^* K^*$ and $\Sigma_c K^*$ channels are very similar. As for the case of $J^P = \frac{3}{2}^-$, the potentials for all the channels except $\Sigma_c^* K$ is attractive. From the figure, one can find that the attraction between Σ_c and K^* is much stronger than the other channels, while the potentials for ΔD_s and ΔD_s^* channels are very similar. There are two channels for the case of $J^P = \frac{5}{2}^-$, which are ΔD_s^* and $\Sigma_c^* K^*$, respectively. Our estimations indicate that the potential for the ΔD_s^* channel is attractive, while the potential for $\Sigma_c^* K^*$ channel is repulsive.

B. Possible bound states

With the above potentials, we can search the $c\bar{s}nnn$ molecular states by the resonating group method (RGM) [99,100], the details of which are present in the Appendix. It should be noted that the number of the basis is limited in the present estimation, thus, one can obtain a solution of $C_{j,L}$ even for a repulsive potential in the single channel estimation. However, the obtained energy in this case should not be the eigenenergy of the bound state since the repulsive potential cannot form a bound state. In this case, the obtained eigenenergies are all above the threshold of the corresponding channels and the eigenenergies are dependent on the basis. When the basis is large enough, the eigenenergies will tend toward the thresholds. In order to discuss the coupled channels effect in the present estimations, we still list these energies in the tables. However, for the bound state, i.e., the estimated eigenenergies are below the threshold, are rather stable with the increasing of basis, which have been further checked in our estimations.

The estimated results are listed in Tables IV and V, which correspond to the states with $I = 1/2$ and $I = 3/2$, respectively. In these tables, E_{sc} and E_{cc} are the eigenenergies of the $c\bar{s}nnn$ molecular states by the single channel estimations and the coupled channel estimations. $E_{th}^{\rm Model}$ and $E_{th}^{\rm Exp}$ stand for the theoretical estimations and experimental measurements of the thresholds of the channels. $E_B = E_{sc} - E_{th}^{\rm Model}$ is the binding energy obtained by the single channel estimations. It should be noticed that in the present work, the relevant parameters were determined by various aspects of the hadron properties. The inaccurateness of the model parameters will lead to the uncertainty of the model predictions. However, compared to the absolute values of the eigenergies, the mass splittings, for example, the E_B, should be more reliable. Additionally, in the present estimations, we define the corrected eigenenergy of the single channel estimations E'_{sc} by $E_{th}^{\rm Exp} + E_B$. In a very similar way, we take the lowest threshold of the involved channels as a scale, we can obtain the corrected eigenenergy of the coupled channel estimations E'_{cc}. In this way, the model dependences of the corrected eigenenergy could be evade to a certain extent.

In addition, it should be mentioned that we mainly search for the possible bound states with the mass below the lowest physical threshold in the present work. These bound state cannot decay via strong interactions, i.e., they are stable against strong decay. Compared to the results of

TABLE IV. The binding energies and the masses of every single channel and those of channel coupling for the pentaquarks with $I = 1/2$. The values are provided in units of MeV.

$I(J^P)$	Channel	E_{sc}	$E_{th}^{\rm Model}$	E_B	$E_{th}^{\rm Exp}$	E'_{sc}	E_{cc}/E_B	E'_{cc}
$\frac{1}{2}(\frac{1}{2}^-)$	ND_s	2954	2957	+3	2907	2910	2784/+3	2784
	ND_s^*	3006	3003	+3	3051	3054		
	$\Lambda_c K$	2785	2781	+4	2781	2785		
	$\Lambda_c K^*$	3104	3100	+4	3178	3182		
	$\Sigma_c K$	2963	2959	+4	2950	2954		
	$\Sigma_c K^*$	3277	3278	−7	3347	3340		
	$\Sigma_c^* K^*$	3283	3303	−20	3412	3392		
$\frac{1}{2}(\frac{3}{2}^-)$	ND_s^*	3006	3003	+3	3051	3054	2985/+1	3016
	$\Lambda_c K^*$	3104	3100	+4	3178	3182		
	$\Sigma_c K^*$	3255	3278	−23	3347	3324		
	$\Sigma_c^* K$	2989	2984	+5	3015	3020		
	$\Sigma_c^* K^*$	3305	3303	+2	3412	3414		
$\frac{1}{2}(\frac{5}{2}^-)$	$\Sigma_c^* K^*$	3283	3303	−20	3412	3392	3283/-20	3392

TABLE V. The binding energies and the masses of every single channel and those of channel coupling for the pentaquarks with $I = 3/2$. The values are provided in units of MeV.

$I(J^P)$	Channel	E_{sc}	E_{th}^{Model}	E_B	E_{th}^{Exp}	E'_{sc}	E_{cc}/E_B	E'_{cc}
$\frac{3}{2}(\frac{1}{2}^-)$	ΔD_s^*	3288	3296	−8	3344	3336	2961/+2	2952
	$\Sigma_c K$	2963	2959	+4	2950	2954		
	$\Sigma_c K^*$	3281	3278	+3	3347	3350		
	$\Sigma_c^* K^*$	3306	3303	+3	3412	3415		
$\frac{3}{2}(\frac{3}{2}^-)$	ΔD_s	3249	3250	−1	3200	3199	2991/+2	3017
	ΔD_s^*	3289	3296	−7	3344	3337		
	$\Sigma_c K^*$	3223	3278	−55	3347	3292		
	$\Sigma_c^* K$	2989	2984	+5	3015	3020		
	$\Sigma_c^* K^*$	3307	3303	+4	3412	3416		
$\frac{3}{2}(\frac{5}{2}^-)$	ΔD_s^*	3291	3296	−5	3344	3339	3259/−32	3307
	$\Sigma_c^* K^*$	3308	3303	+5	3412	3417		

bound states estimations, the mass shift of every resonance state is not very large, which indicates that the scattering channel and bound-state channel coupling effect is not very strong. The reason is that the mass difference between the scattering channel and bound-state channel is large, about 100–300 MeV.

For the system with $I(J^P) = \frac{1}{2}(\frac{1}{2}^-)$, the single channel calculations indicate that $\Sigma_c K^*$ and $\Sigma_c^* K^*$ can be bound states with the binding energies to be 7 MeV and 20 MeV, respectively. From Fig. 1, one can find that the $\Sigma_c K^*$ and $\Sigma_c^* K^*$ channels have strong attractive interactions, thus it is not surprising to obtain the bound states in these two channels and the RGM estimations are consistent with the expectations of the effective potential analysis. In addition, the estimations in Ref. [67] indicated that $\Sigma_c K^*$ with $I(J^P) = \frac{1}{2}(\frac{1}{2}^-)$ could be a good candidate of charmed-strange molecular state, which is consistent with our single channel estimations. However, for the ND_s and ND_s^* channel, the QDCSM estimations indicate that the attractions are rather weak, and the eigenenergies obtained by single channel estimations are above the threshold of ND_s and ND_s^*, respectively. As for $\Lambda_c K$, $\Lambda_c K^*$, and $\Sigma_c K$ channels, the potentials are repulsive, and thus the obtained eigenenergies of these channels are all above the corresponding thresholds. After considering the coupled channel effect, the obtained energy for $I(J^P) = \frac{1}{2}(\frac{1}{2}^-)$ pentaquark state is 2784 MeV, which is still above the threshold of the lowest physical channel $\Lambda_c K$, which indicates that there is no below-threshold $c\bar{s}nnn$ pentaquark state with $I(J^P) = \frac{1}{2}(\frac{1}{2}^-)$.

Furthermore, the potentials of the $\Sigma_c K^*$ and $\Sigma_c^* K^*$ channels are attractive, and single-channel estimations also indicate that there are bound states in these two channels with their masses to be above the lowest threshold, thus, these states can decay into the corresponding channels. After including the coupled channel effect, these two bound states may become the resonance states. To confirm this possibility, we further investigate the scattering process of the open channels to search the resonance states, which will be discussed in the next subsection.

For the system with $I(J^P) = \frac{1}{2}(\frac{3}{2}^-)$, there are five channels, which are ND_s^*, $\Lambda_c K^*$, $\Sigma_c K^*$, $\Sigma_c^* K$ and $\Sigma_c^* K^*$, respectively. The single-channel estimations indicate that the $\Sigma_c K^*$ can be bounded with a binding energy of −23 MeV due to the deep attractive interaction between Σ_c and K^*. Nevertheless, we do not obtain a bound state in the ND_s^* and $\Sigma_c^* K^*$ channel because their attractive interactions are not strong enough. Noted that the eigenenergy of this system is 3016 MeV after including the coupled channel effects, which is still higher than the threshold of the lowest channel $\Sigma_c^* K$ as shown in Table IV. For the system with $I(J^P) = \frac{1}{2}(\frac{5}{2}^-)$, it includes only one channel, which is $\Sigma_c^* K^*$. From Fig. 1, one can find the attractive interaction between Σ_c^* and K^* is very strong, which leads to a bound state of $\Sigma_c^* K^*$ with the binding energy of −20 MeV.

For the system with $I(J^P) = \frac{3}{2}(\frac{1}{2}^-)$, the strong attractive interaction between Δ and D_s^* leads to a bound state of ΔD_s^* with the binding energy of 8 MeV, while in the other channels, the single channel estimations indicate the pentaquark states are all above the corresponding threshold. When considering the coupled channel effect, the eigenenergy of the $c\bar{s}nnn$ pentaquark with $I(J^P) = \frac{3}{2}(\frac{1}{2}^-)$ is 2952 MeV, which is about 2 MeV above the threshold of the lowest channel $\Sigma_c K$. For the system with $I(J^P) = \frac{3}{2}(\frac{3}{2}^-)$, there are five channels as shown in Table V. The single-channel calculations demonstrate that there are three bound states, which are ΔD_s, ΔD_s^* and $\Sigma_c K^*$, and their binding energy are −1, −7, and −55 MeV, respectively. This conclusion is consistent with the behavior of the effective potential as shown in Fig. 2. Besides, these three bound states can decay into some open channels, and we can further check the nature of these bound states in the scattering of these open channels, which are presented in the next subsection. Moreover, the coupled channel estimations indicate that the lowest energy of $c\bar{s}nnn$ pentaquark states with $I(J^P) = \frac{3}{2}(\frac{3}{2}^-)$ is 3019 MeV,

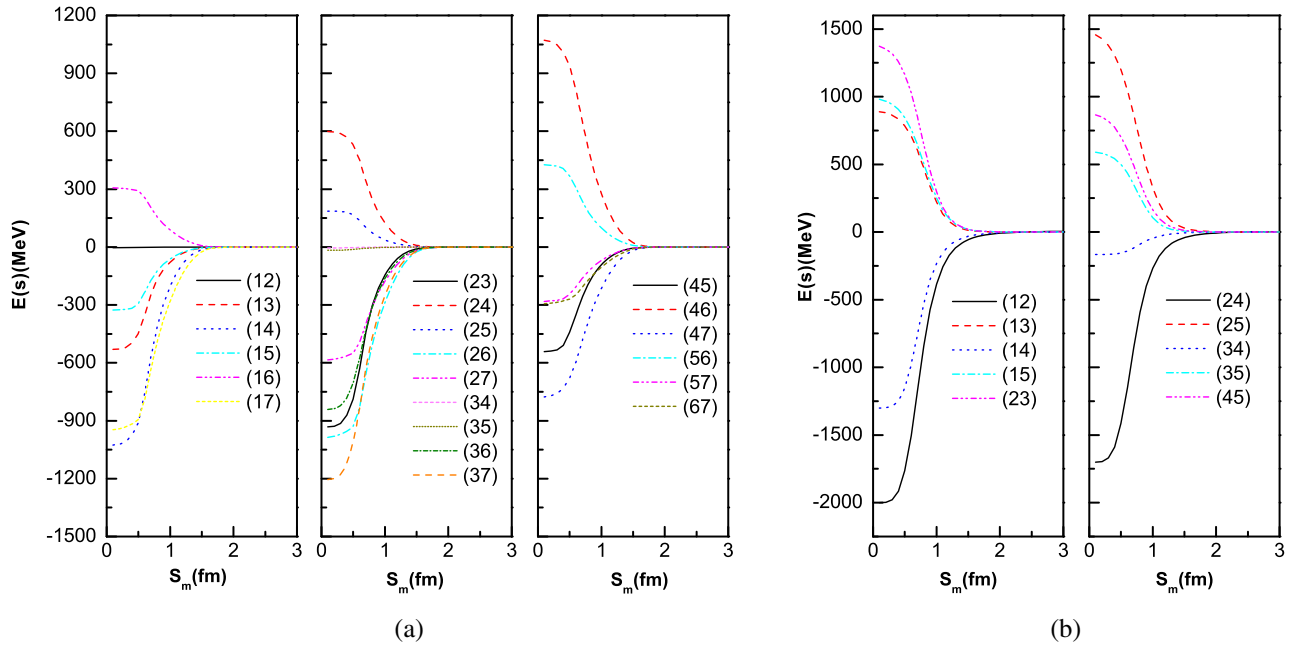

FIG. 3. The transition potentials defined in Eq. (12) for different channels of the charmed-strange pentaquark systems with $I = 1/2$ in QDCSM. (a) 1, 2, 3, 4, 5, 6, and 7 stand for ND_s, ND_s^*, $\Lambda_c K$, $\Sigma_c^* K^*$, $\Lambda_c K^*$, $\Sigma_c K$, and $\Sigma_c K^*$; (b) 1, 2, 3, 4, and 5 stand for ND_s^*, $\Lambda_c K^*$, $\Sigma_c K^*$, $\Sigma_c^* K$, and $\Sigma_c^* K^*$.

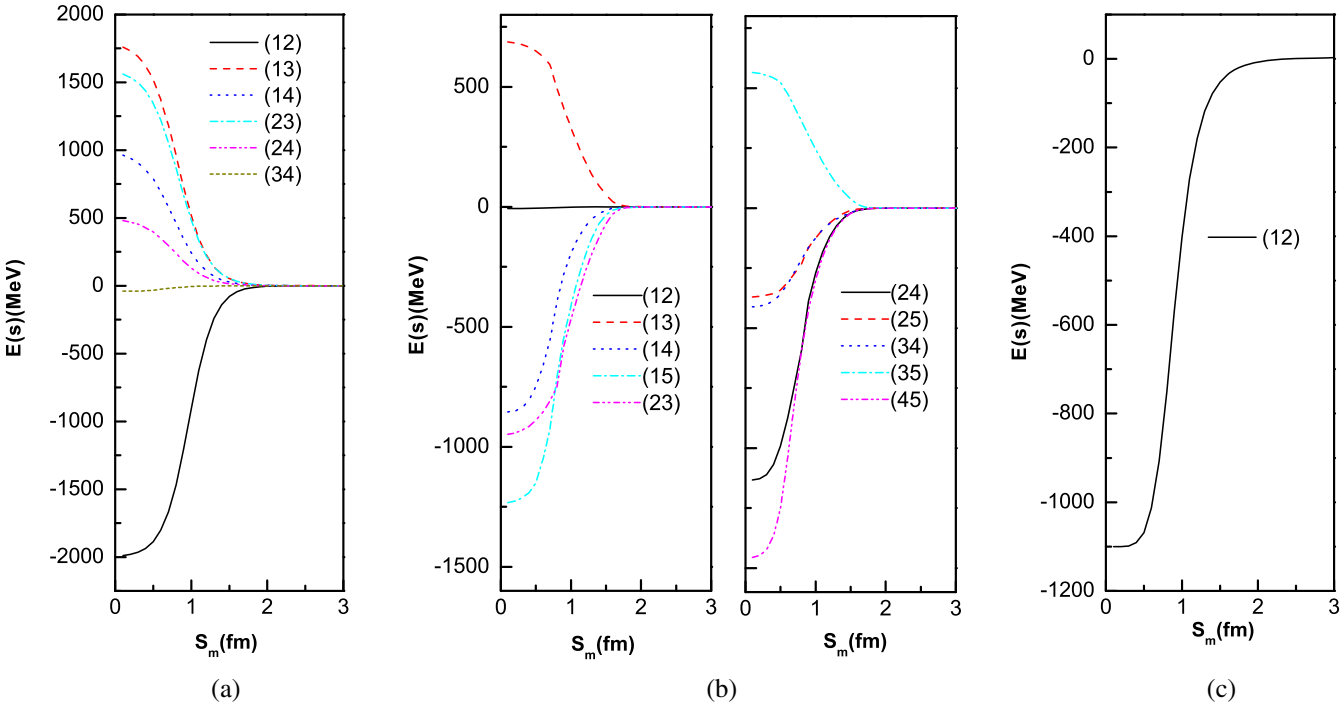

FIG. 4. The transition potentials defined in Eq. (12) different channels of the charmed-strange pentaquark systems with $I = 3/2$ in QDCSM. (a) 1, 2, 3, and 4 represents channels $\Sigma_c^* K^*$, $\Sigma_c K^*$, $\Sigma_c K$, and ΔD_s^*; (b) 1, 2, 3, 4, and 5 stand for ΔD_s, ΔD_s^*, $\Sigma_c K^*$, $\Sigma_c^* K$, and $\Sigma_c^* K^*$; (c) 1 and 2 stand for ΔD_s^* and $\Sigma_c^* K^*$.

which is higher than the threshold of the lowest physical channel $\Sigma_c^* K$. For the system with $I(J^P) = \frac{3}{2}(\frac{5}{2}^-)$, the single-channel calculations indicate that ΔD_s^* is a bound state with a binding energy of -5 MeV, and the energy of $\Sigma_c^* K^*$ is 3417 MeV, which is 5 MeV higher than the corresponding threshold. Furthermore, a bound state with the binding energy of -37 MeV is obtained by the coupled channel estimations.

As previously noted, channel coupling effects can significantly impact the outcomes of a system. In the present systems, the coupling between the calculated S-wave channels occurs via central force. To better understand the strength of channel coupling, we have computed the transition potentials for these channels, as illustrated in Figs. 3 and 4. For instance, we have taken the $I(J^P) = \frac{3}{2}(\frac{5}{2}^-)$ system as an example. Figure 4(c) displays the transition potentials for two channels, namely ΔD_s^* and $\Sigma_c^* K^*$. It is evident that the strong coupling among these channels results in the binding of ΔD_s^*.

In the above RGM calculations, we obtain two bound states in the $c\bar{s}nnn$ pentaquark system with $I(J^P) = \frac{1}{2}(\frac{5}{2}^-)$ and $\frac{3}{2}(\frac{5}{2}^-)$, respectively. To further check the possibility of those bound states, the low-energy scattering phase shifts of these channels are investigated by the variational method. The details of this method can be found in the Appendix. The scattering length a_0, the effective range r_0, and the binding energy E_B' are calculated, which are presented in Table VI. From Table VI, one can find the scattering length of $\Sigma_c^* K^*$ and ΔD_s^* are all positive, and the binding energy obtained by the variational method, E_B', of those two states is close to the binding energy E_B obtained by RGM calculations, which further confirm the existence of bound states. Moreover, from Fig. 5, it is obvious that the low-energy phase shifts of the $\Sigma_c^* K^*$ with $I(J^P) = \frac{1}{2}(\frac{5}{2}^-)$ and ΔD_s^* with $I(J^P) = \frac{3}{2}(\frac{5}{2}^-)$ in the coupled channel estimations can reach up to 180 degrees at $E_{c.m} \sim 0$ and decreases rapidly with $E_{c.m}$ increasing. Such behaviors also indicate the existence of bound states.

C. Possible resonance states

As indicated above, some bound states can be obtained in the single-channel calculation due to the attractive interactions between hadron pairs. These states can decay into the corresponding open channels, which may lead to some resonance states. To further check the existence of the resonance states, we studied the scattering phase shifts of all possible open channels in the QDCSM, which are shown in Figs. 6 and 7. In addition, the mass and width of the possible resonance states are also calculated and listed in Table VII. The current calculation applies only to the decay of S-wave open channels due to the negligible widths of the higher partial waves.

TABLE VI. The the scattering length a_0, the effective range r_0 and the binding energy E_B' determined by the variation method.

$I(J^P)$	Channel	a_0 (fm)	r_0 (fm)	E_B' (MeV)
$\frac{1}{2}(\frac{5}{2}^-)$	$\Sigma_c^* K^*$	2.06	0.98	−23.8
$\frac{3}{2}(\frac{5}{2}^-)$	ΔD_s^*	2.00	1.00	−34.7

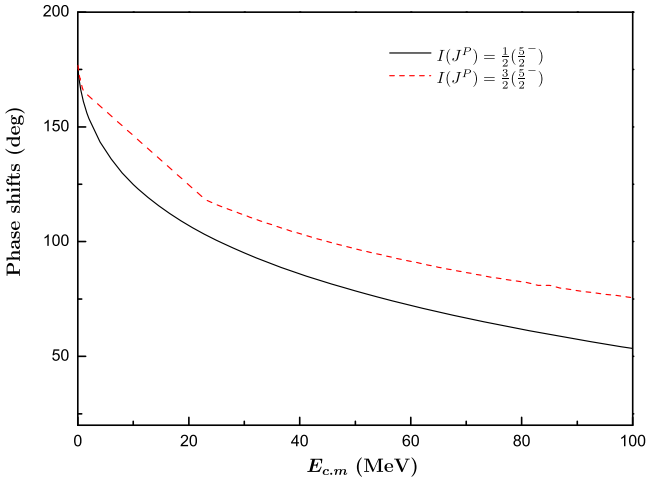

FIG. 5. The phase shifts of the $\Sigma_c^* K^*$ with $I(J^P) = \frac{1}{2}(\frac{5}{2}^-)$ and ΔD_s^* with $I(J^P) = \frac{3}{2}(\frac{5}{2}^-)$ in the coupled channel estimations.

For the $I(J^P) = \frac{1}{2}(\frac{1}{2}^-)$, our estimations demonstrate that two bound states, $\Sigma_c K^*$ and $\Sigma_c^* K^*$, are available in the single channel calculations. According to Table IV, the possible decay channels of these two bound states are ND_s, ND_s^*, $\Lambda_c K$, $\Lambda_c K^*$, and $\Sigma_c K$. So we analyze the scattering phase shifts of three-channel coupling with two bound states and one of the corresponding open channels. From Fig. 6(a), one can find there is no resonance state in the scattering phase shifts of ND_s and $\Lambda_c K$ channels, but the phase shifts of the ND_s^*, $\Lambda_c K^*$, and $\Sigma_c K$ channels indicate that there is one resonance state, which means that there is a $\Sigma_c K^*$ resonance in these three channels. On the contrary, the $\Sigma_c^* K^*$ bound state vanishes due to the channel coupling effect pushing it above the threshold. The resonance mass and decay width can be obtained from the shape of the resonance. Here, in order to minimize the theoretical errors and compare our predictions with future experimental data, we shift the resonance mass by $m_R = M - E_{th} + E_{\rm exp}$. The estimated masses and widths of the resonances in different channels are listed in Table VII, which is $m_R = (3342\text{–}3346)$ MeV and $\Gamma_R = 25.5$ MeV. From Table VII, one can find that the mass shifts of the resonance mass in the different channels are small, which indicates that the scattering channel and bound state channel coupling effect is not strong due to the large mass difference between the scattering channel and bound state channel.

For the states with $I(J^P) = \frac{1}{2}(\frac{3}{2}^-)$, the $\Sigma_c K^*$ bound state can decay into three open channels, which are ND_s^*, $\Lambda_c K^*$, and $\Sigma_c^* K$, respectively. The scattering phase shifts of two-channel coupling with a bound state channel and one of the open channels are calculated, and the results are shown in

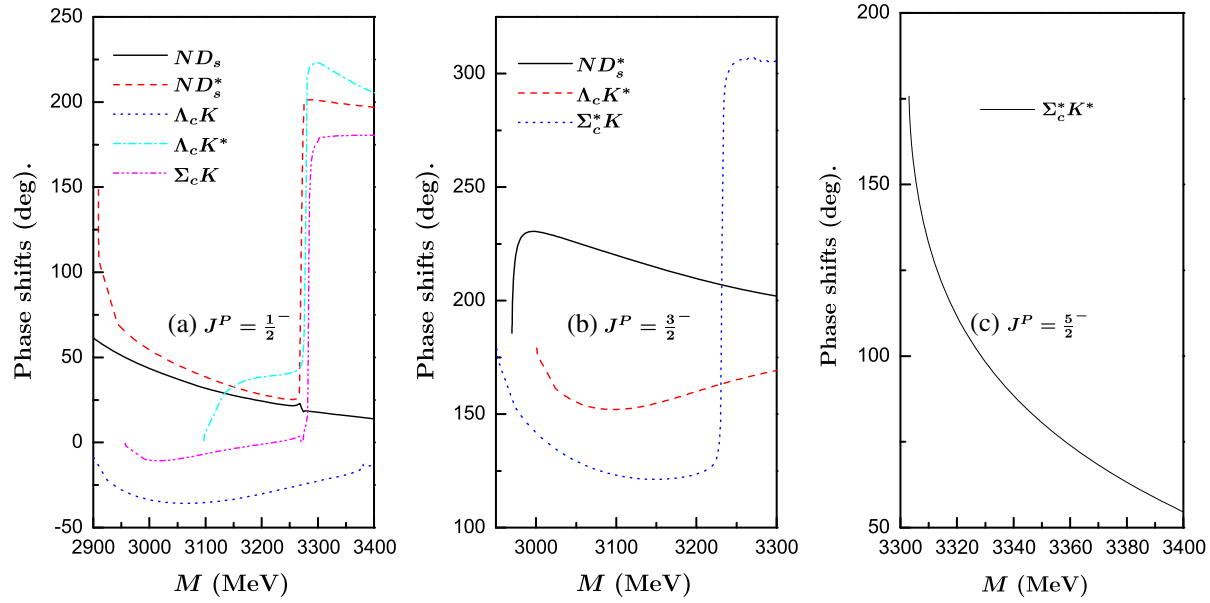

FIG. 6. The phase shifts of the open channels with $I = 1/2$ in QDCSM depending on the sum of the corresponding theoretical threshold of the open channel and the incident energy.

Fig. 6(b). The $\Sigma_c K^*$ resonance state can be found in the scattering phase shifts of $\Sigma_c^* K$ but not in scattering phase shifts of other channels. From Table VII, the resonance mass and decay widths are estimated to be 3333 and 3.3 MeV, respectively. For the state with $I(J^P) = \frac{1}{2}(\frac{5}{2}^-)$, there is only one channel. From Fig. 6(c), one can find that the phase shift is close to 180° as $M \sim 0$ MeV, which implies that this state is a bound state rather than a resonant state when we only consider the scattering process under S-wave, which further confirmed the existence of $\Sigma_c^* K^*$ bound states with $I(J^P) = \frac{1}{2}(\frac{5}{2}^-)$.

For the $c\bar{s}qqq$ pentaquark states with $I = 3/2$, the behavior of the scattering phase shifts of the open channel is presented in Fig. 7. There is only one bound state, ΔD_s^*, in the single-channel calculation with the binding energy of -8 MeV for $J^P = 1/2$ system. This bound state can decay into the open channel $\Sigma_c K$. From the analysis the scattering phase shifts of $J^P = \frac{1}{2}^-$ in Fig. 7(a), one can find a ΔD_s^*

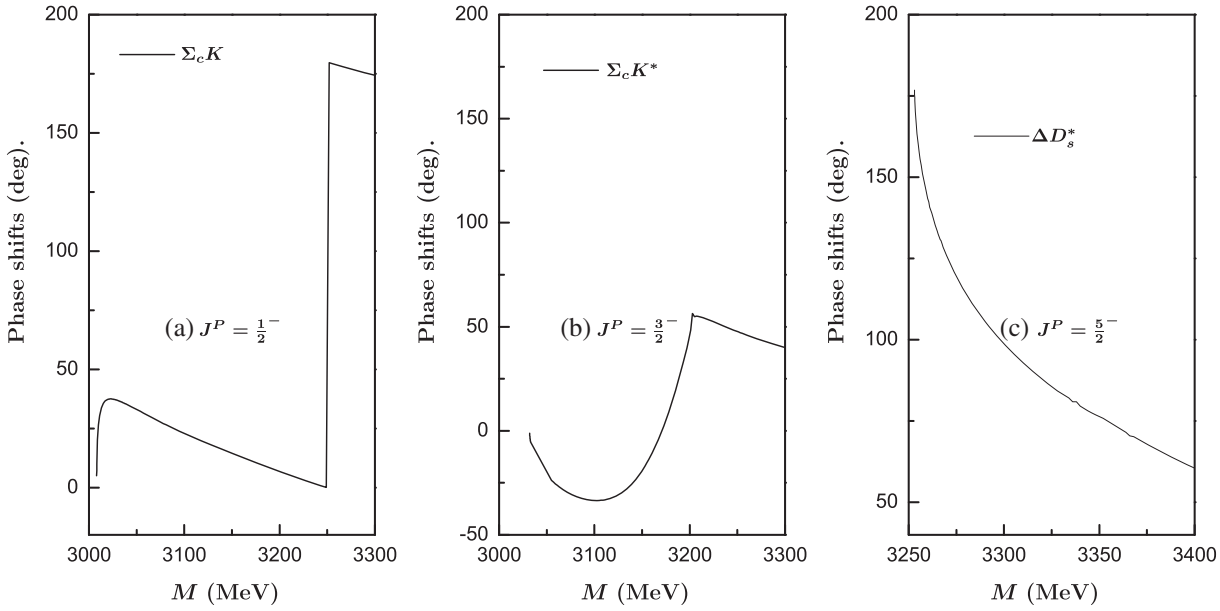

FIG. 7. The phase shifts of the open channels with $I = 3/2$ in QDCSM depending on the sum of the corresponding theoretical threshold of the open channel and the incident energy.

TABLE VII. The masses and decay widths (in the unit of MeV) of resonance states with the difference scattering process. m_R stands for the modified resonance mass. Γ is the partial decay width of the resonance state decaying to an open channel. $\Gamma_{\rm Total}$ is the total decay width of the resonance state.

	Three channel coupling			
	$I(J^P)=\frac{1}{2}(\frac{1}{2}^-)$		$I(J^P)=\frac{1}{2}(\frac{1}{2}^-)$	
	$\Sigma_c K^*$		$\Sigma_c^* K^*$	
Open channels	m_R	Γ	m_R	Γ
ND_s	⋯	⋯	⋯	⋯
ND_s^*	3344	5.1	⋯	⋯
$\Lambda_c K$	⋯	⋯	⋯	⋯
$\Lambda_c K^*$	3346	1.4	⋯	⋯
$\Sigma_c K$	3342	19	⋯	⋯
$\Gamma_{\rm Total}$		25.5		

	Two channel coupling			
	$I(J^P)=\frac{1}{2}(\frac{3}{2}^-)$		$I(J^P)=\frac{3}{2}(\frac{1}{2}^-)$	
	$\Sigma_c K^*$		ΔD_s^*	
Open channels	m_R	Γ	m_R	Γ
ND_s^*	⋯	⋯	⋯	⋯
$\Lambda_c K^*$	⋯	⋯	⋯	⋯
$\Sigma_c K$	⋯	⋯	3343	0.01
$\Sigma_c^* K$	3333	3.3	⋯	⋯
$\Gamma_{\rm Total}$		3.3		0.01

resonance state in $\Sigma_c K$ channel with a mass and width of 3343 and 0.01 MeV, respectively. For the $J^P=\frac{3}{2}^-$ system, the single channel estimations find three bound states, which are ΔD_s, ΔD_s^* and $\Sigma_c K^*$, respectively. These bound states can only decay into the open channel $\Sigma_c^* K$. So in the present work, a four-channel coupling estimation is considered. From Fig. 7(b), no resonance states appear in the scattering phase shifts of $\Sigma_c^* K$, which reveals that the bound states ΔD_s, ΔD_s^* and $\Sigma_c K^*$ become scattering states through the four-channel coupling. For the $J^P=\frac{5}{2}^-$ system, although the ΔD_s^* is a bound state in the single-channel calculation, this channel cannot decay into $\Sigma_c^* K^*$ due to the kinematic limit. The phase shifts of ΔD_s^* is presented in Fig. 7(c), the behavior of which is similar to that of the $\Sigma_c^* K^*$ with $I(J^P)=\frac{1}{2}(\frac{5}{2}^-)$, which indicates the bound state nature of ΔD_s^*.

It should be noted that Δ-baryon and K^* meson are broad resonances with widths on the order of 100 MeV and approximately 50 MeV, respectively. The Δ baryon dominantly decays into $N\pi$, while the K^* meson dominantly decays into $K\pi$, and accordingly the three body decays should have significant contributions to the widths of the resonance states. Thus, the resonance states predicted in the present estimations should be much broader.

IV. SUMMARY

Recently, the LHCb Collaboration reported their observations of the $T^a_{c\bar{s}0}(2900)^{++}$ and $T^a_{c\bar{s}0}(2900)^0$ in the $D_s^+\pi^\pm$ invariant mass spectrums. Inspired by these newly discovered exotic states candidates, we investigate the charmed-strange pentaquark states $c\bar{s}nnn$ by using the RGM in the framework of QDCSM. Herein, the effective potentials are estimated to explore the interactions of individual channels in different $I(J^P)$ quantum numbers systems. The single channel and coupled channels calculations are carried out to find the possible bound states. Our estimations show that there are two bound states for the charmed-strange pentaquark system with $I(J^P)$ quantum numbers to be $\frac{1}{2}(\frac{5}{2}^-)$ and $\frac{3}{2}(\frac{5}{2}^-)$, respectively. The masses are estimated to be 3392 MeV for the pentaquark state with $\frac{1}{2}(\frac{5}{2}^-)$ and 3307 MeV for the state with $\frac{3}{2}(\frac{5}{2}^-)$.

Apart from the bound states, the scattering phase shifts are also estimated to search for the possible resonance states. The present estimations indicate that there are three resonance states in the $c\bar{s}nnn$ pentaquark system. The $\Sigma_c K^*$ resonance state with $I(J^P)=\frac{1}{2}(\frac{1}{2}^-)$ can be found in the scattering phase shifts of ND_s^*, $\Lambda_c K^*$ and $\Sigma_c K$ channels, and the mass and width are (3342–3346) MeV and 25.5 MeV, respectively. The $\Sigma_c K^*$ resonance state with $I(J^P)=\frac{1}{2}(\frac{3}{2}^-)$ can be observed in the $\Sigma_c^* K$ channel with the mass and width to be 3333 and 3.3 MeV, respectively. In addition, a ΔD^* resonance state with $I(J^P)=\frac{3}{2}(\frac{1}{2}^-)$ is also visible in the scattering phase shift of the $\Sigma_c K$ channel, and the mass and width of this resonance state are 3343 and 0.01 MeV, respectively.

ACKNOWLEDGMENTS

This work is supported partly by the National Natural Science Foundation of China under Contracts No. 12175037, No. 12335001, No. 11775118, No. 11535005, No. 12205249, No. 12205125, and No. 11865019, and is also supported by the Fundamental Research Funds for the Central Universities No. 2242022R20040; and the China Postdoctoral Science Foundation No. 2021M690626 and No. 1107020201. Besides, Jiangsu Provincial Natural Science Foundation Project (No. BK20221166), National Youth Fund: No. 12205125 and School-Level Research Projects of Yancheng Institute of Technology (No. xjr2022039) also supported this work.

APPENDIX: RESONATING GROUP METHOD FOR BOUND STATE AND SCATTERING PROBLEMS

In the present work, We perform bound state calculations as well as scattering calculations for the $N\overline{D_s}$ system by using the RGM in QDCSM. The issue of this approach is how to deal with the two-body problem. In this method, when dealing with the two-cluster system, one can only

consider the relative motion between the clusters, while the two clusters are frozen inside. So the wave function of the baryon-meson system is

$$\psi = \sum_L \mathcal{A}[[\hat{\phi}_A(\boldsymbol{\rho_A}, \boldsymbol{\lambda_A})\hat{\phi}_B(\boldsymbol{\rho_B})]^{[\sigma]IS} \otimes \chi_L(\mathbf{R}_{AB})]^J, \quad \text{(A1)}$$

where L stands for the orbital angular momentum and the symbol $\mathcal{A}$ is the antisymmetry operator, which can be defined as

$$\mathcal{A} = 1 - P_{14} - P_{24} - P_{34}, \quad \text{(A2)}$$

where 1, 2, and 3 stand for the quarks in the baryon cluster, and 4 stands for the quark in the meson cluster. $\hat{\phi}_A$ and $\hat{\phi}_B$ are the internal cluster wave functions of the baryon A and meson B:

$$\hat{\phi}_A = \left(\frac{2}{3\pi b^2}\right)^{3/4}\left(\frac{1}{2\pi b^2}\right)^{3/4} e^{-(\frac{\rho_A^2}{4b^2}+\frac{\lambda_A^2}{3b^2})}\eta_{I_A} S_A \xi_A^c, \quad \text{(A3)}$$

$$\hat{\phi}_B = \left(\frac{1}{2\pi b^2}\right)^{3/4} e^{-\frac{\rho_B}{4b^2}}\eta_{I_B} S_B \xi_B^c, \quad \text{(A4)}$$

where η_I, S, and ξ represent the flavor, spin, and internal color terms of the cluster wave functions, respectively. ρ_A and λ_A are the internal coordinates for the baryon cluster A and ρ_B is the internal coordinate for the meson cluster B. The Jacobi coordinates are defined as follows:

$$\begin{aligned}
&\boldsymbol{\rho_A} = \boldsymbol{r_1} - \boldsymbol{r_2}, \qquad \boldsymbol{\rho_B} = \boldsymbol{r_4} - \boldsymbol{r_5},\\
&\boldsymbol{\lambda_A} = \boldsymbol{r_3} - \frac{1}{2}(\mathbf{r}_1 + \mathbf{r}_2),\\
&\boldsymbol{R_A} = \frac{1}{3}(\boldsymbol{r_1} + \boldsymbol{r_2} + \boldsymbol{r_3}), \qquad \boldsymbol{R_B} = \frac{1}{2}(\boldsymbol{r_4} + r_5),\\
&\boldsymbol{R_{AB}} = \boldsymbol{R_A} - \boldsymbol{R_B}, \qquad \boldsymbol{R_G} = \frac{3}{5}\boldsymbol{R_A} + \frac{2}{5}\boldsymbol{R_B}. \quad \text{(A5)}
\end{aligned}$$

From the variational principle, after variation with respect to the relative motion wave function $\chi(R) = \sum_L \chi_L(R)$, one obtains the RGM equation,

$$\int H(\boldsymbol{R}, \boldsymbol{R}')\chi(\boldsymbol{R}')d(R') = E\int N(\boldsymbol{R}, \boldsymbol{R}')\chi(\boldsymbol{R}')d(R'), \quad \text{(A6)}$$

where $H(\boldsymbol{R}, \boldsymbol{R}')$ and $N(\boldsymbol{R}, \boldsymbol{R}')$ are Hamiltonian and norm kernels, respectively. The eigenenergy E and the wave functions are obtained by solving the RGM equation.

Generally, one can introduce generator coordinates S_m to expand the Lth relative motion wave function $\chi_L(\boldsymbol{R})$ by,[4]

$$\begin{aligned}
\chi_L(\boldsymbol{R}) &= \frac{1}{\sqrt{4\pi}}\left(\frac{6}{5\pi b^2}\right)^{3/4}\sum_{m=1}^{n} C_m\\
&\quad\times\int \exp\left[-\frac{3}{5b^2}(\boldsymbol{R} - \boldsymbol{S}_m)^2\right] Y^L(\hat{\boldsymbol{S}}_m)d\hat{\boldsymbol{S}}_m\\
&= \sum_{m=1}^{n} C_m \frac{u_L(\boldsymbol{R}, \boldsymbol{S}_m)}{\boldsymbol{R}} Y^L(\hat{\boldsymbol{R}}), \quad \text{(A7)}
\end{aligned}$$

with

$$\begin{aligned}
u_L(\boldsymbol{R}, \boldsymbol{S}_m) &= \sqrt{4\pi}\left(\frac{6}{5\pi b^2}\right)^{3/4}\mathbf{R}\, e^{-\frac{3}{5b^2}(\boldsymbol{R}-\boldsymbol{S}_m)^2}\\
&\quad\times m^L j_L\left(-i\frac{6}{5b^2}S_m\right), \quad \text{(A8)}
\end{aligned}$$

where C_m is expansion coefficients, n is the number of the Gaussian bases, which is determined by the stability of the results, and j_L is the Lth spherical Bessel function. Then the relative motion wave function $\chi(\mathbf{R})$ is

$$\begin{aligned}
\chi(\boldsymbol{R}) &= \frac{1}{\sqrt{4\pi}}\sum_L\left(\frac{6}{5\pi b^2}\right)^{3/4}\\
&\quad\times\sum_{m=1}^{n} C_m\int e^{-\frac{3}{5b^2}(\mathbf{R}-\mathbf{S}_m)^2} Y^L(\hat{\boldsymbol{S}}_m)d\hat{\boldsymbol{S}}_m. \quad \text{(A9)}
\end{aligned}$$

After the inclusion of the center of mass motion,

$$\Phi_G(\mathbf{R}_G) = \left(\frac{5}{\pi b^2}\right)^{3/4} e^{-\frac{5}{2b^2}\mathbf{R}_G}, \quad \text{(A10)}$$

the total wave function in Eq. (A1) can be rewritten as,

$$\begin{aligned}
\Psi_{5q} &= \mathcal{A}\sum_{m,L} C_{m,L}\int \frac{1}{\sqrt{4\pi}}\prod_{\alpha=1}^{3}\Phi_\alpha(S_m)\prod_{\beta=4}^{5}\Phi_\beta(-S_m)\\
&\quad\times[[\eta_{I_A S_A}\eta_{I_B S_B}]^{IS} Y^L(\hat{\mathbf{S}}_m)]^J[\xi_c(A)\xi_c(B)]^{[\sigma]}, \quad \text{(A11)}
\end{aligned}$$

where $\Phi_\alpha(S_m)$ and $\Phi_\beta(-S_m)$ are the single-particle orbital wave function with different reference centers, for which the specific form can be seen in Eq. (11).

With the reformulated ansatz as shown in Eq. (A11), the RGM equation becomes an algebraic eigenvalue equation,

$$\sum_{j,L} C_{J,L} H_{i,j}^{L,L'} = E\sum_j C_{j,L'} N_{i,j}^{L'}, \quad \text{(A12)}$$

where $N_{i,j}^{L'}$ and $H_{i,j}^{L,L'}$ are the overlap of the wave functions and the matrix elements of the Hamiltonian, respectively. By solving the generalized eigenvalue problem, we can obtain the energies of the pentaquark E and the corresponding expansion coefficient $C_{j,L}$. Finally, the relative

[4]In the present estimation, only the S-wave bound state is considered, i.e., $L = 0$.

motion wave function between two clusters can be obtained by substituting the $C_{j,L}$ into Eq. (A7).

For a scattering problem, the relative wave function is expanded as

$$\chi_L(\mathbf{R}) = \sum_{m=1}^{n} C_m \frac{\tilde{u}_L(\boldsymbol{R}, \boldsymbol{S}_m)}{\boldsymbol{R}} Y^L(\hat{\boldsymbol{R}}), \tag{A13}$$

with

$$\tilde{u}_L(\boldsymbol{R}, \boldsymbol{S}_m) = \begin{cases} \alpha_m u_L(\boldsymbol{R}, \boldsymbol{S}_m), & \boldsymbol{R} \leq \boldsymbol{R}_C \\ [h_L^-(\boldsymbol{k}, \boldsymbol{R}) - s_m h_L^+(\boldsymbol{k}, \boldsymbol{R})] R_{AB}, & \boldsymbol{R} \geq \boldsymbol{R}_C \end{cases}, \tag{A14}$$

where u_L is presented Eq. (A8), $h_L^{\pm}$ is the Lth spherical Hankel functions, $\boldsymbol{k}$ is the momentum of the relative motion with $\boldsymbol{k} = \sqrt{2\mu E_{ie}}$, μ is the reduced mass of two hadrons of the open channel, E_{ie} is the incident energy of the relevant open channels, which can be written as $E_{ie} = E_{\text{total}} - E_{th}$ with E_{total} and E_{th} denote the total energy and the threshold of open channel, respectively. $\boldsymbol{R}_C$ is a cutoff radius beyond which all the strong interaction can be disregarded. Besides, α_m and s_m are complex parameters that are determined by the smoothness condition at $\boldsymbol{R} = \boldsymbol{R}_C$ and C_m satisfy $\Sigma_{m=1}^{n} C_m = 1$. After performing the variational procedure, a Lth partial-wave equation for the scattering problem can be deduced as,

$$\sum_{m=1}^{n} \mathcal{L}_{im}^L C_m = \mathcal{M}_i^L (i = 0, 1, \ldots, n-1), \tag{A15}$$

with

$$\mathcal{L}_{im}^L = \mathcal{K}_{im}^L - \mathcal{K}_{i0}^L - \mathcal{K}_{0m}^L + \mathcal{K}_{00}^L, \tag{A16}$$

$$\mathcal{M}_i^L = \mathcal{K}_{00}^L - \mathcal{K}_{i0}^L, \tag{A17}$$

and

$$\mathcal{K}_{im}^L = \left\langle \hat{\phi}_A \hat{\phi}_B \frac{\tilde{u}_L(\boldsymbol{R}', \boldsymbol{S}_m)}{\boldsymbol{R}'} Y^L(\boldsymbol{R}') | H - E | \right. \tag{A18}$$

$$\left. \times \mathcal{A} \left[\hat{\phi}_A \hat{\phi}_B \frac{\tilde{u}_L(\boldsymbol{R}, \boldsymbol{S}_m)}{\boldsymbol{R}} Y^L(\boldsymbol{R}) \right] \right\rangle. \tag{A19}$$

By solving Eq. (A15), we can obtain the expansion coefficients C_m, then the S-matrix element S_L and the phase shifts δ_L are given by

$$S_L = |S_L| e^{2i\delta_L} = \sum_{m=1}^{n} C_m s_m. \tag{A20}$$

Finally, the cross section can be obtained from the scattering phase shifts by the formula,

$$\sigma_L = \frac{4\pi}{k^2} (2L+1) \sin^2 \delta_L. \tag{A21}$$

Based on the single-channel scattering calculation discussed above, we can also to take into account the coupled channels effect. First, we can write the total wave function as

$$\Psi^{(c)} = \sum_{\gamma} \mathcal{A}_\gamma [\hat{\Phi}_\gamma(\hat{\xi}) \chi_\gamma^{(c)}(R_\gamma)], \qquad c = (\alpha, \beta), \tag{A22}$$

where γ represents all two-body channels. The asymptotic behavior of $\chi_\gamma^{(c)}(R_\gamma)$ is,

$$\chi_\gamma^{(c)}(R_\gamma) = \chi_\gamma^{(-)}(\kappa_\gamma, R_\gamma) \delta_{\gamma c} + S_{\gamma c} \chi_\gamma^{(+)}(\kappa_\gamma, R_\gamma), \quad R_\gamma > R_\gamma^{(c)}, \tag{A23}$$

where $S_{\gamma c}$ means the S-matrix element of $c \to \gamma$; $\chi_\gamma^{(\pm)}$ can be written as

(i) for the open channel

$$\chi_\gamma^{(\pm)}(\kappa_\gamma, R_\gamma) = \frac{1}{\sqrt{\nu_\gamma}} h_{L_\gamma}^{(\pm)}(\kappa_\gamma, R_\gamma), \qquad R_\gamma > R_\gamma^{(c)}, \tag{A24}$$

(ii) for the close channel

$$\chi_\gamma^{(\pm)}(\kappa_\gamma, R_\gamma) = W_{L_\gamma}^{(\pm)}(\kappa_\gamma, R_\gamma), \quad R_\gamma > R_\gamma^{(c)}, \tag{A25}$$

where ν_γ is the relative rate of motion, $\nu_\gamma = h\kappa_\gamma/\mu_\gamma$, κ_γ, and μ_γ stand for the momentum of the relative motion with γ channels and the reduced mass of the two hadrons. Besides, the discussion of $W_{L_\gamma}^{(\pm)}(\kappa_\gamma, R_\gamma)$ can be found in Ref. [100].

Similar to the single channel scattering phase shift approach, we first introduce the trial wave function $\Psi_t^{(c)}$:

$$\Psi_t^{(c)} = \sum_{\gamma} \mathcal{A}_\gamma [\Phi_\gamma(\hat{\xi}) \chi_{\gamma,t}^{(c)}(R_\gamma)] + \sum_{\nu}^{(c)} \Omega_{\nu,t}, c = (\alpha, \beta), \tag{A26}$$

where $\Omega_{\nu,t}$ denotes the decay amplitude without the forward term. $\chi_{\gamma,t}^{(c)}(R_\gamma)$ is the trial wave function for the relative motion orbit, which can be written as

$$\chi_{\gamma,t}^{(c)}(R_\gamma) = \chi_\gamma^{(-)}(\kappa_\gamma, R_\gamma) \delta_{\gamma c} + S_{\gamma c,t} \chi_\gamma^{(+)}(\kappa_\gamma, R_\gamma), \quad R_\gamma > R_\gamma^{(c)} \tag{A27}$$

Here, $\chi_{\gamma,t}^{(c)}(R_\gamma)$ can be expanded with a series of known wave functions:

$$\chi^{(c)}_{\gamma,t}(R_\gamma) = \sum_{i=0}^{n\gamma} C^{(c)}_{\gamma i}\chi_{\gamma i}(R_\gamma), \qquad (c=\alpha,\beta) \tag{A28}$$

with

$$\chi_{\gamma i}(R_\gamma) = \begin{cases} p_{\gamma i}\chi^{\text{in}}_{\gamma i}(R_\gamma), & R_\gamma \le R^c_\gamma, \\ \chi^{(-)}_\gamma(\kappa_\gamma, R_\gamma) + s_{\gamma i}\chi^{+}_\gamma(\kappa_\gamma, R_\gamma), & R_\gamma \ge R^c_\gamma. \end{cases} \tag{A29}$$

Because $\chi_{\gamma i}(R_\gamma)$ is a continuous wave function, the wave function and the derivative of the wave function are also continuous at $R_\gamma = R^c_\gamma$,

$$p_{\gamma i}\chi^{\text{in}}_{\gamma i}(R^c_\gamma) = \chi^{(-)}_\gamma(\kappa_\gamma, R^c_\gamma) + s_{\gamma i}\chi^{+}_\gamma(\kappa_\gamma, R^c_\gamma), \tag{A30}$$

$$p_{\gamma i}\frac{d}{dR_\gamma}\chi^{\text{in}}_{\gamma i}(R_\gamma)|_{R_\gamma=R^c_\gamma} = \frac{d}{dR_\gamma}[\chi^{(-)}_\gamma(\kappa_\gamma, R_\gamma) - s_{\gamma i}\chi^{(+)}_\gamma(\kappa_\gamma, R_\gamma)]_{R_\gamma=R^c_\gamma}, \tag{A31}$$

so $p_{\gamma i}$ and $s_{\gamma i}$ can be obtained. According to the Eqs. (A27)–(A29), we can obtain

$$\sum_{i=0}^{n\gamma} C^{(c)}_{\gamma i} = \delta_{\gamma c}, \qquad (c=\alpha,\beta) \tag{A32}$$

and

$$\sum_{i=0}^{n\gamma} C^{(c)}_{\gamma i} s_{\gamma i} = S_{\gamma c,t}.(c=\alpha,\beta) \tag{A33}$$

In the same way as when calculating the single channel, we end up with two systems of linear equations

$$\sum_{\delta}\sum_{j=1}^{n\delta} L_{\gamma i,\delta j}C^c_{\delta j} + \Sigma_\mu L_{\gamma i,\mu}b^c_\mu = M^{(c)}_{\gamma i} \tag{A34}$$

$$\sum_{\delta}\sum_{j=1}^{n\delta} L_{\nu,\delta j}C^c_{\delta j} + \Sigma_\mu L_{\nu,\mu}b^c_\mu = M^{(c)}_{\nu}, \tag{A35}$$

where $L_{\gamma i,\delta j}$, $L_{\gamma i,\mu}$, $L_{\nu,\delta j}$, and $L_{\nu,\mu}$, whose expressions can be found in Ref. [100]. By solving the system of Eqs. (A34) and (A35), $C^{(c)}_{\gamma,i}$ and $b^{(c)}_\nu$ can be obtained, and then substituting into Eq. (A33), we can obtained the approximate S-matrix element $S_{\gamma c,t}$. Finally based on the single channel scattering approach, the S-matrix element $S_{\beta\alpha,st}$ can be written as

$$S_{\beta\alpha,st} = S_{\beta\alpha,t} - \frac{i\kappa^2}{hb}\left[\sum_\gamma\sum_{i=0}^{n\gamma} K_{\beta 0,\gamma i}C^\alpha_{\gamma i} + \Sigma_\nu K_{\beta 0,\nu}b^{(\alpha)}_\nu\right], \tag{A36}$$

where $K_{\beta 0,\gamma i}$ and $K_{\beta 0,\nu}$ can be found Ref. [100].

Next how to obtain the scattering phase shifts needs to be discussed in different cases. Take two channels coupling as an example, if one of these two channels is an open channel and the other is a closed channel, then we study the scattering phase shifts after this open channel is affected by the closed channel, and we can use Eq. (A20) to get the scattering phase shifts. For the better understanding, we take $\Delta D^*_s + \Sigma_c K$ channel coupling calculation with $I(J^P) = \frac{3}{2}(\frac{1}{2}^-)$ as an example. Here ΔD^*_s is the resonance state and $\Sigma_c K$ is the open channel. In the scattering phase shifts calculation of $\Sigma_c K$ without incorporating ΔD^*_s channel, the phase shifts will be a a smooth curve, the phase shift varies gently with the increasing incident energy. However, as shown Fig. 7(a), the phase shifts of $\Sigma_c K$ show a structure in the $\Delta D^*_s + \Sigma_c K$ two-channel coupling calculation, the phase shifts will rise rapidly at some energies. the change will exceed 180°. The incident energy corresponding to the phase shift at 90° is the energy of the resonance state, and the difference between the two incident energies corresponding to the 45° and 135° of the phase shifts is the decay width.

If there are two open channels, we can use the above method to calculate four matrix elements: S_{11}, S_{12}, S_{21}, and S_{22}. These four elements can be arranged into a 2×2 matrix, which can be diagonalized to obtain two eigenvalues, representing the S-matrix elements of the two open channels. These eigenvalues can be substituted into Eq. (A20) to obtain the scattering phase shifts of the two channels.

In addition, based on Eq. (A20), we can obtain the scattering length a_0 and the effective range r_0 at the low-energy scattering phase shift by,

$$k\cot\delta_L = -\frac{1}{a_0} + \frac{1}{2}r_0k^2 + O(k^4), \tag{A37}$$

where $k = \sqrt{2\mu E_{c.m}}$, μ and $E_{c.m}$ are the reduced mass of two hadrons and the incident energy, respectively.

According to above results, the wave number α can be available by the relation [101],

$$r_0 = \frac{2}{\alpha}\left(1 - \frac{1}{\alpha a_0}\right). \tag{A38}$$

Finally, the binding energy E'_B is calculated according to the relation,

$$E'_B = \frac{\hbar^2\alpha^2}{2\mu}. \tag{A39}$$

[1] M. Gell-Mann, Phys. Lett. **8**, 214 (1964).
[2] R. L. Jaffe, Phys. Rev. Lett. **38**, 195 (1977); **38**, 617(E) (1977).
[3] S. K. Choi *et al.* (Belle Collaboration), Phys. Rev. Lett. **91**, 262001 (2003).
[4] M. Ablikim *et al.* (BESIII Collaboration), Phys. Rev. Lett. **110**, 252001 (2013).
[5] Z. Q. Liu *et al.* (Belle Collaboration), Phys. Rev. Lett. **110**, 252002 (2013); **111**, 019901(E) (2013).
[6] H. X. Chen, W. Chen, X. Liu, and S. L. Zhu, Phys. Rep. **639**, 1 (2016).
[7] E. S. Swanson, Phys. Rep. **429**, 243 (2006).
[8] M. B. Voloshin, Prog. Part. Nucl. Phys. **61**, 455 (2008).
[9] R. Chen, X. Liu, and S. L. Zhu, Nucl. Phys. **A954**, 406 (2016).
[10] A. Esposito, A. Pilloni, and A. D. Polosa, Phys. Rep. **668**, 1 (2017).
[11] R. F. Lebed, R. E. Mitchell, and E. S. Swanson, Prog. Part. Nucl. Phys. **93**, 143 (2017).
[12] F. K. Guo, C. Hanhart, U. G. Meißner, Q. Wang, Q. Zhao, and B. S. Zou, Rev. Mod. Phys. **90**, 015004 (2018).
[13] B. Aubert *et al.* (*BABAR* Collaboration), Phys. Rev. Lett. **90**, 242001 (2003).
[14] B. Aubert *et al.* (*BABAR* Collaboration), Phys. Rev. Lett. **93**, 181801 (2004).
[15] D. Besson *et al.* (CLEO Collaboration), Phys. Rev. D **68**, 032002 (2003); **75**, 119908(E) (2007).
[16] P. Krokovny *et al.* (Belle Collaboration), Phys. Rev. Lett. **91**, 262002 (2003).
[17] Y. Mikami *et al.* (Belle Collaboration), Phys. Rev. Lett. **92**, 012002 (2004).
[18] B. Aubert *et al.* (*BABAR* Collaboration), Phys. Rev. D **69**, 031101 (2004).
[19] B. Aubert *et al.* (*BABAR* Collaboration), Phys. Rev. D **74**, 032007 (2006).
[20] M. Ablikim *et al.* (BESIII Collaboration), Phys. Rev. D **97**, 051103 (2018).
[21] H. Y. Cheng and W. S. Hou, Phys. Lett. B **566**, 193 (2003).
[22] Y. Q. Chen and X. Q. Li, Phys. Rev. Lett. **93**, 232001 (2004).
[23] H. Kim and Y. Oh, Phys. Rev. D **72**, 074012 (2005).
[24] M. Nielsen, R. D. Matheus, F. S. Navarra, M. E. Bracco, and A. Lozea, Nucl. Phys. B, Proc. Suppl. **161**, 193 (2006).
[25] K. Terasaki, arXiv:hep-ph/0512285.
[26] Z. G. Wang and S. L. Wan, Nucl. Phys. **A778**, 22 (2006).
[27] C.-J. Xiao, D. Y. Chen, and Y. L. Ma, Phys. Rev. D **93**, 094011 (2016).
[28] T. Barnes, F. E. Close, and H. J. Lipkin, Phys. Rev. D **68**, 054006 (2003).
[29] F. S. Navarra, M. Nielsen, E. Oset, and T. Sekihara, Phys. Rev. D **92**, 014031 (2015).
[30] E. E. Kolomeitsev and M. F. M. Lutz, Phys. Lett. B **582**, 39 (2004).
[31] J. Hofmann and M. F. M. Lutz, Nucl. Phys. **A733**, 142 (2004).
[32] F. K. Guo, P. N. Shen, H. C. Chiang, R. G. Ping, and B. S. Zou, Phys. Lett. B **641**, 278 (2006).
[33] Y. J. Zhang, H. C. Chiang, P. N. Shen, and B. S. Zou, Phys. Rev. D **74**, 014013 (2006).
[34] J. L. Rosner, Phys. Rev. D **74**, 076006 (2006).
[35] F. K. Guo, P. N. Shen, and H. C. Chiang, Phys. Lett. B **647**, 133 (2007).
[36] M. Z. Liu, X. Z. Ling, L. S. Geng, En-Wang, and J. J. Xie, Phys. Rev. D **106**, 114011 (2022).
[37] Z. Yang, G. J. Wang, J. J. Wu, M. Oka, and S. L. Zhu, Phys. Rev. Lett. **128**, 112001 (2022).
[38] P. G. Ortega, J. Segovia, D. R. Entem, and F. Fernandez, Phys. Rev. D **94**, 074037 (2016).
[39] R. Aaij *et al.* (LHCb Collaboration), Phys. Rev. Lett. **125**, 242001 (2020).
[40] R. Aaij *et al.* (LHCb Collaboration), Phys. Rev. D **102**, 112003 (2020).
[41] Z. G. Wang, Int. J. Mod. Phys. A **35**, 2050187 (2020).
[42] X. G. He, W. Wang, and R. Zhu, Eur. Phys. J. C **80**, 1026 (2020).
[43] J. R. Zhang, Phys. Rev. D **103**, 054019 (2021).
[44] G. J. Wang, L. Meng, L. Y. Xiao, M. Oka, and S. L. Zhu, Eur. Phys. J. C **81**, 188 (2021).
[45] M. Z. Liu, J. J. Xie, and L. S. Geng, Phys. Rev. D **102**, 091502 (2020).
[46] H. X. Chen, W. Chen, R. R. Dong, and N. Su, Chin. Phys. Lett. **37**, 101201 (2020).
[47] Y. Huang, J. X. Lu, J. J. Xie, and L. S. Geng, Eur. Phys. J. C **80**, 973 (2020).
[48] R. Molina and E. Oset, Phys. Lett. B **811**, 135870 (2020).
[49] Y. Xue, X. Jin, H. Huang, and J. Ping, Phys. Rev. D **103**, 054010 (2021).
[50] Q. F. Lü, D. Y. Chen, and Y. B. Dong, Phys. Rev. D **102**, 074021 (2020).
[51] S. S. Agaev, K. Azizi, and H. Sundu, J. Phys. G **48**, 085012 (2021).
[52] H. Mutuk, J. Phys. G **48**, 055007 (2021).
[53] C. J. Xiao, D. Y. Chen, Y. B. Dong, and G. W. Meng, Phys. Rev. D **103**, 034004 (2021).
[54] J. He and D. Y. Chen, Chin. Phys. C **45**, 063102 (2021).
[55] X. H. Liu, M. J. Yan, H. W. Ke, G. Li, and J. J. Xie, Eur. Phys. J. C **80**, 1178 (2020).
[56] T. J. Burns and E. S. Swanson, Phys. Lett. B **813**, 136057 (2021).
[57] T. Gershon (LHCb Collaboration), arXiv:2206.15233.
[58] https://indico.cern.ch/event/1176505/.
[59] LHCb Collaboration, Phys. Rev. Lett. **131**, 041902 (2023).
[60] J. B. Cheng, S. Y. Li, Y. R. Liu, Y. N. Liu, Z. G. Si, and T. Yao, Phys. Rev. D **101**, 114017 (2020).
[61] R. M. Albuquerque, S. Narison, D. Rabetiarivony, and G. Randriamanatrika, Nucl. Phys. **A1007**, 122113 (2021).
[62] T. J. Burns and E. S. Swanson, Phys. Rev. D **103**, 014004 (2021).
[63] S. S. Agaev, K. Azizi, and H. Sundu, Phys. Lett. B **820**, 136530 (2021).
[64] K. Azizi and U. Özdem, Phys. Rev. D **104**, 114002 (2021).
[65] H. W. Ke, Y. F. Shi, X. H. Liu, and X. Q. Li, Phys. Rev. D **106**, 114032 (2022).
[66] J. Wei, Y. H. Wang, C. S. An, and C. R. Deng, Phys. Rev. D **106**, 096023 (2022).
[67] R. Chen and Q. Huang, arXiv:2208.10196.
[68] S. S. Agaev, K. Azizi, and H. Sundu, J. Phys. G **50**, 055002 (2023).
[69] F. X. Liu, R. H. Ni, X. H. Zhong, and Q. Zhao, Phys. Rev. D **107**, 096020 (2023).

[70] Y. H. Ge, X. H. Liu, and H. W. Ke, Eur. Phys. J. C **82**, 955 (2022).
[71] Z. L. Yue, C. J. Xiao, and D. Y. Chen, Phys. Rev. D **107**, 034018 (2023).
[72] R. Molina and E. Oset, Phys. Rev. D **107**, 056015 (2023).
[73] Q. Qin, J. L. Qiu, and F. S. Yu, Eur. Phys. J. C **83**, 227 (2023).
[74] H. T. An, Z. W. Liu, F. S. Yu, and X. Liu, Phys. Rev. D **106**, L111501 (2022).
[75] A. De Rujula, H. Georgi, and S. L. Glashow, Phys. Rev. D **12**, 147 (1975).
[76] N. Isgur and G. Karl, Phys. Rev. D **20**, 1191 (1979).
[77] N. Isgur and G. Karl, Phys. Rev. D **19**, 2653 (1979); **23**, 817(E) (1981).
[78] N. Isgur and G. Karl, Phys. Rev. D **18**, 4187 (1978).
[79] F. Wang, G. h. Wu, L. j. Teng, and J. T. Goldman, Phys. Rev. Lett. **69**, 2901 (1992).
[80] L. Chen, H. Pang, H. Huang, J. Ping, and F. Wang, Phys. Rev. C **76**, 014001 (2007).
[81] M. Chen, H. Huang, J. Ping, and F. Wang, Phys. Rev. C **83**, 015202 (2011).
[82] G. H. Wu, L. J. Teng, J. L. Ping, F. Wang, and J. T. Goldman, Phys. Rev. C **53**, 1161 (1996).
[83] H. Huang, P. Xu, J. Ping, and F. Wang, Phys. Rev. C **84**, 064001 (2011).
[84] F. Wang, D. Qing, P. Xu, and J. L. Ping, Nucl. Phys. **A631**, 462C (1998).
[85] H. Huang, C. Deng, J. Ping, and F. Wang, Eur. Phys. J. C **76**, 624 (2016).
[86] H. Huang, J. Ping, and F. Wang, Phys. Rev. C **89**, 035201 (2014).
[87] X. Liu, D. Chen, H. Huang, J. Ping, X. Chen, and Y. Yang, Sci. China Phys. Mech. Astron. **66**, 221012 (2023).
[88] M. Tanabashi *et al.* (Particle Data Group), Phys. Rev. D **98**, 030001 (2018).
[89] J. Vijande, F. Fernandez, and A. Valcarce, J. Phys. G **31**, 481 (2005).
[90] F. Fernandez and E. Oset, Nucl. Phys. **A455**, 720 (1986).
[91] G. h. Wu, J. L. Ping, L. j. Teng, F. Wang, and J. T. Goldman, Nucl. Phys. **A673**, 279 (2000).
[92] J. L. Ping, F. Wang, and J. T. Goldman, Nucl. Phys. **A657**, 95 (1999).
[93] H. R. Pang, J. L. Ping, F. Wang, and J. T. Goldman, Phys. Rev. C **65**, 014003 (2002).
[94] F. Huang and W. L. Wang, Phys. Rev. D **98**, 074018 (2018).
[95] M. Xu, M. Yu, and L. Liu, Phys. Rev. Lett. **100**, 092301 (2008).
[96] Z. Xia, S. Fan, X. Zhu, H. Huang, and J. Ping, Phys. Rev. C **105**, 025201 (2022).
[97] H. Huang, J. Ping, X. Zhu, and F. Wang, Eur. Phys. J. C **82**, 805 (2022).
[98] J. L. Ping, F. Wang, and J. T. Goldman, Phys. Rev. C **65**, 044003 (2002).
[99] M. Kamimura, Nucl. Phys. **A351**, 456 (1981).
[100] M. Kamimura, Prog. Theor. Phys. Suppl. **62**, 236 (1977).
[101] V. A. Babenko and N. M. Petrov, Phys. At. Nucl. **66**, 1319 (2003).